Validated Spectral Angle Mapper Algorithm for Geological Mapping: Comparative Study between Quickbird and Landsat-TM

G.Girouard [1], A.Bannari [1], A. El Harti [2] and A. Desrochers [3]

[1] Remote Sensing and Geomatics of the Environment Laboratory
Department of Geography, University of Ottawa, Ottawa-Carleton GeoScience Center
P.O. Box 450, Ottawa (Ontario) K1N 6N5
Tel: (613) 562-5800 (ext. 1042), Fax: (613) 562-5145
E-mail: abannari@uottawa.ca
[2] Remote Sensing and GIS Applied to Geosciences and the Environment
Faculty of Science and Techniques Beni-Mellal, Morocco, University of Cadi Ayyad
[3] Department of Earth Science, University of Ottawa
Ottawa-Carleton GeoScience Center

KEY WORDS – Geology, Mapping, Exploration, Landsat, Quickbird, DEM, GIS

ABSTRACT:

The aim of this study is to validate the Spectral Angle Mapper (SAM) algorithm for geological mapping in Central Jebilet Morocco and compare the results between high and medium spatial resolution sensors, such as Quickbird and Landsat TM respectively. The geology of the study area is dominated by the Sahrlef schist, which is intruded by numerous bodies of acidic and basic magmatic rocks and lens-shaped pyrrhotite stratabound massive deposits. The results show that SAM of TM data can provide mineralogical maps that compare favorably with ground truth and known surface geology maps. Even do, Quickbird has a high spatial resolution compared to TM; its data did not provide good results for SAM because of the low spectral resolution.

1. Introduction

Multispectral remote sensing techniques have been widely used in the past decades to discriminate different materials based on the dissimilarity that exist among their spectral properties (Hunt *et al.*, 1971). Geological applications could greatly take advantage of this technology because it allows observing and mapping the surface of the Earth over large areas, but the generally low spectral resolution of multispectral sensors obstruct geological research. Digital image classification is a technique that is widely used to classify each individual pixel in an image based on the spectral information in order to create lithological or geological maps. Various classification algorithms have been used in the past decades in a variety of applications for mapping: forestry, agriculture, land use, geology etc. The main disadvantage of these algorithms is that each pixel in the image is compared to the training site signatures identified by the analyst and labeled as the class it most closely "resembles" digitally. Spectral Angle Mapper (SAM) is different from these standard classification methods because it compares each pixel in the image with every endmember for each class and assigns a ponderation value between 0 (low resemblance) and 1 (high resemblance). Endmembers can be taken directly from the image or from signatures measured directly in the field or laboratory. The main disadvantage of these algorithms, including SAM, is that they do not consider the sub-pixel value. The spectral mixture problem can become problematic because most of the Earth's surface is heterogeneous, thus for a medium space resolution sensor like Landsat TM, false assumptions can be made. Nonetheless, SAM has been used successfully in the past for geological mapping and for identifying potential mineral exploration sites with the use of the "USGS Spectral Library"
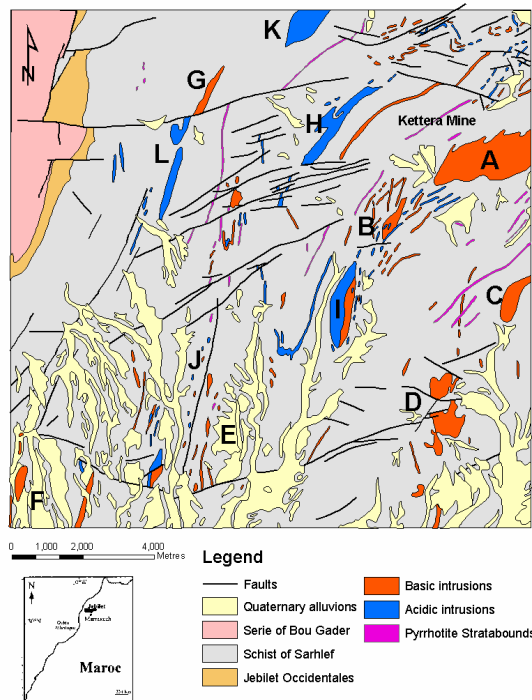
as reference spectrum (Crosta *et al.*, 1998). McCubbin *et al.* (1998) used SAM to map alteration minerals associated with mine waste and Van der Meer *et al.* (1997) used this technique for mapping different ophiolite lithologies in Cyprus. The purpose of this paper is to discuss and to validate the results for the geological mapping of Central Jebilet in Morocco using SAM algorithm with two different optical sensors such as Landsat TM and Quickbird. These two sensors possess spatial and spectral characteristics that are opposite to each other. Landsat TM has a medium spatial resolution (30 x 30 meters) versus the high spatial resolution (2.5 x 2.5 meters) for Quickbird. Nonetheless, the spectral dimension of TM is richer for geological mapping than Quickbird, because it has 6 bands that cover the spectrum between 0.45-2.35 µm in opposition to 4 bands for Quickbird that only cover the 0.45-0.90 µm range.

2. Materials and Methods

2.1. Geological Setting

The study area is located in the Paleozoic terrain of central Jebilet in Morocco, which is about 8 Km north of Marrakech (8º20'W - 7º40'W; 31º40'N - 32ºN). The topography of the area is formed of small-elongated hills, which vary from 350 to 750 meters in elevation. The total area covered by this study is 100 Km^2 and is characterized by a lithological diversity, semi-desert environment, significant mineral potential and consistent geological setting. The geology of central Jebilet is composed of four main rock units of which the Sahrlef schist is the dominant rock unit. It is intensively deformed and intruded by numerous acidic and basic magmatic bodies. The economic

interest of the area is focused on lens-shaped pyrrhotite stratabound massive deposits (iron caps), which appear on the surface as rust-colored oxidized minerals caused by the oxidation of iron sulphides.

Figure 1 – Simplified geological map of Central Jebilet (Huvelin, 1970)

2.2. Data
Two images were used in this study. First of all, the Landsat TM image was acquired on June 26th 1987 and the Quickbird image on February 26th 2003. Both images were acquired over the same area and at the same solar time, thus have similar illumination characteristics. They also show low vegetation distribution, which is good for geological and lithological mapping.

2.3. Pre-processing
Various factors affect the signal measured at the sensor, such as drift of the sensor radiometric calibration, atmospheric and topographical effects. For accurate analysis, all of these corrections are necessary for remote sensing imagery. The images were corrected from atmospheric effects using the updated Herman transfer radiative code (H5S) adapted by Teillet and Santer (1991). H5S simulates the signal received at the top of the atmosphere from a surface reflecting solar and sky irradiance at sea level while considering terrain elevation

and the sensor altitude (Teillet and Santer 1991). Radiometric corrections on TM were done with the TM post-calibration dynamics ranges and the solar exoatmospheric spectral irradiance values (Clark, 1986). The image distributors did radiometric corrections on the Quickbird image. Topographical effects were corrected on both images (orthorectification) using a digital elevation model (DEM) derived from a topographic map using a digitizing table and a geographic information system (GIS) tool. A 30 x 30 meter grid was created for TM and a 2.5 x 2.5 meter grid for Quickbird.

2.4 Spectral Angle Mapper algorithm (SAM)
The SAM is a classification method that permits rapid mapping by calculating the spectral similarity between the image spectrums to reference reflectance spectra (Yuhas *et al.*, 1992; Kruse *et al.*, 1993; Van der Meer *et al.*, 1997; Crosta *et al.,* 1998; De Carvalho and Meneses, 2000; Schwarz and Staenz, 2001; Hunter and Power, 2002). The reference spectra can either be taken from laboratory or field measurements or extracted directly from the image. SAM measures the spectral similarity by calculating the angle between the two spectra, treating them as vectors in *n*-dimensional space (Kruse et *al.,* 1993; Van der Meer et *al.,* 1997; Rowan and Mars., 2003). Small angles between the two spectrums indicate high similarity and high angles indicate low similarity.

This method is not affected by solar illumination factors, because the angle between the two vectors is independent of the vectors length (Crosta et *al.*, 1998; Kruse et *al.*, 1993). It takes the arccosine of the dot product between the test spectrums "*t*" to a reference spectrum "*r*" with the following equation (Yuhas *et al.*, 1992; Kruze et *al.*, 1993; Van der Meer et *al.,* 1997; De Carvalho and Meneses, 2000):

$$\alpha = \cos^{-1}\left(\frac{\sum_{i=1}^{nb} t_i r_i}{\left(\sum_{i=1}^{nb} t_i^2\right)^{1/2}\left(\sum_{i=1}^{nb} r_i^2\right)^{1/2}} \right) \quad (1)$$

Where nb = the number of bands
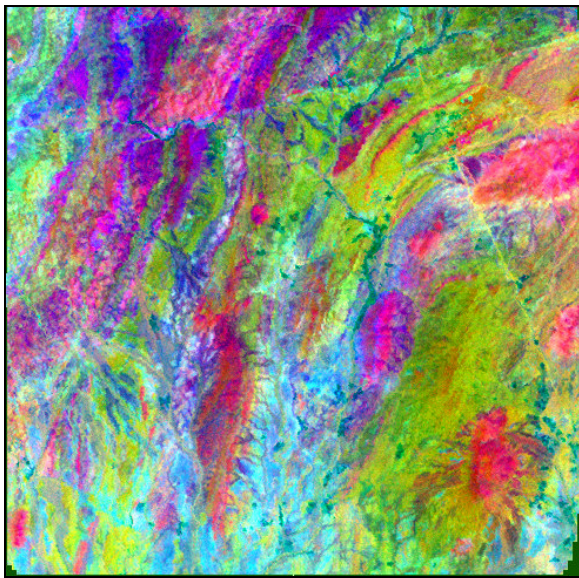t_i = test spectrum
r_i = reference spectrum

The main advantages of the SAM algorithm are that its an easy and rapid method for mapping the spectral similarity of image spectra to reference spectra. It is also a very powerful classification method because it represses the influence of shading effects to accentuate the target reflectance characteristics (De Carvalho and Meneses, 2000). The main disadvantage of this method is the spectral mixture problem. The most erroneous assumption made with SAM is the supposition that endmembers chosen to classify the image represent the pure spectra of a reference material. This problem generally occurs with medium spatial resolution images, such as Landsat TM. The surface of the Earth is complex and heterogeneous in many ways, thus having mixed pixels is incontestable. The spectral confusion in pixels can lead to underestimation and overestimation errors for a spectral class. In general, the spectral mixture problem should decrease with higher resolution images like Quickbird. But in some cases, it can also increase the mixture problem because more local

variations in the spectral property of a surface become more apparent, such as humidity, elevation and shading effects (Gebbinck, 1998).
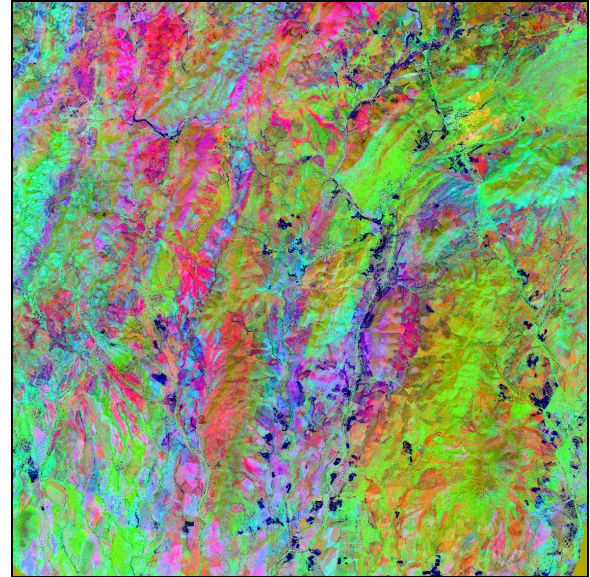
2.5 Endmember selection

Image endmember's for Landsat TM and Quickbird were selected through visualizing spectral scatter plots of image band combinations using ENVI system. A Principal Component (PC) transformation was used to guide image endmember selection since it puts almost 90% of the variances on the first two components and minimizes the influence of band to band correlation (Small, 2003, Wu and Murray, 2003). After examination of figures 2A and 2B, it is obvious that TM is spectrally richer than Quickbird. Important lithologies, as shown in the geological map (figure 1), such as the basic and acidic magmatic bodies and the iron caps are much more perceptible in the TM image. Quickbird does not have any spectral bands between 1.55 and 2.35 µm and this area of the spectrum is essential for geological discrimination.

As illustrated in figure 3A, a total of 8 endmembers were extracted from the TM image such as basic and acidic magmatic rocks, iron caps, schists, carbonates, Quaternary deposits, sandy loams and finally vegetation. These endmembers were all significantly different from each other, thus could be used with confidence for classification. The carbonate endmember was selected in the TM image where it was observed in the field with GPS coordinates. For Quickbird (figure 3B), the same endmembers were chosen, but the carbonate unit was neglected because it had low separability with several other endmembers, which would have given bad results for the classification.

B

Figure 2 – PCA color composite for Landsat TM (A) and Quickbird (B) (PC 3 = Red, PC 2 = Green and PC 1 = Blue).
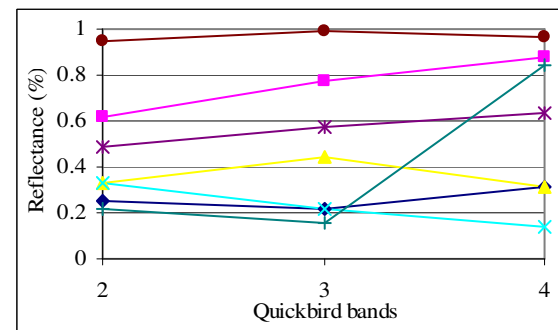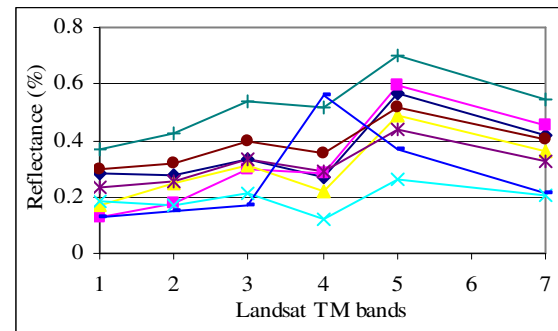

A

Figure 3 – Endmembers for TM and Quickbird

3. Results and Discussion

3.1 SAM for Landsat TM

A

B

C

D - Output Legend

Unclassified
Basic intrusions   Iron caps
Sandy loams   Carbonates
Acidic intrusions   Vegetation
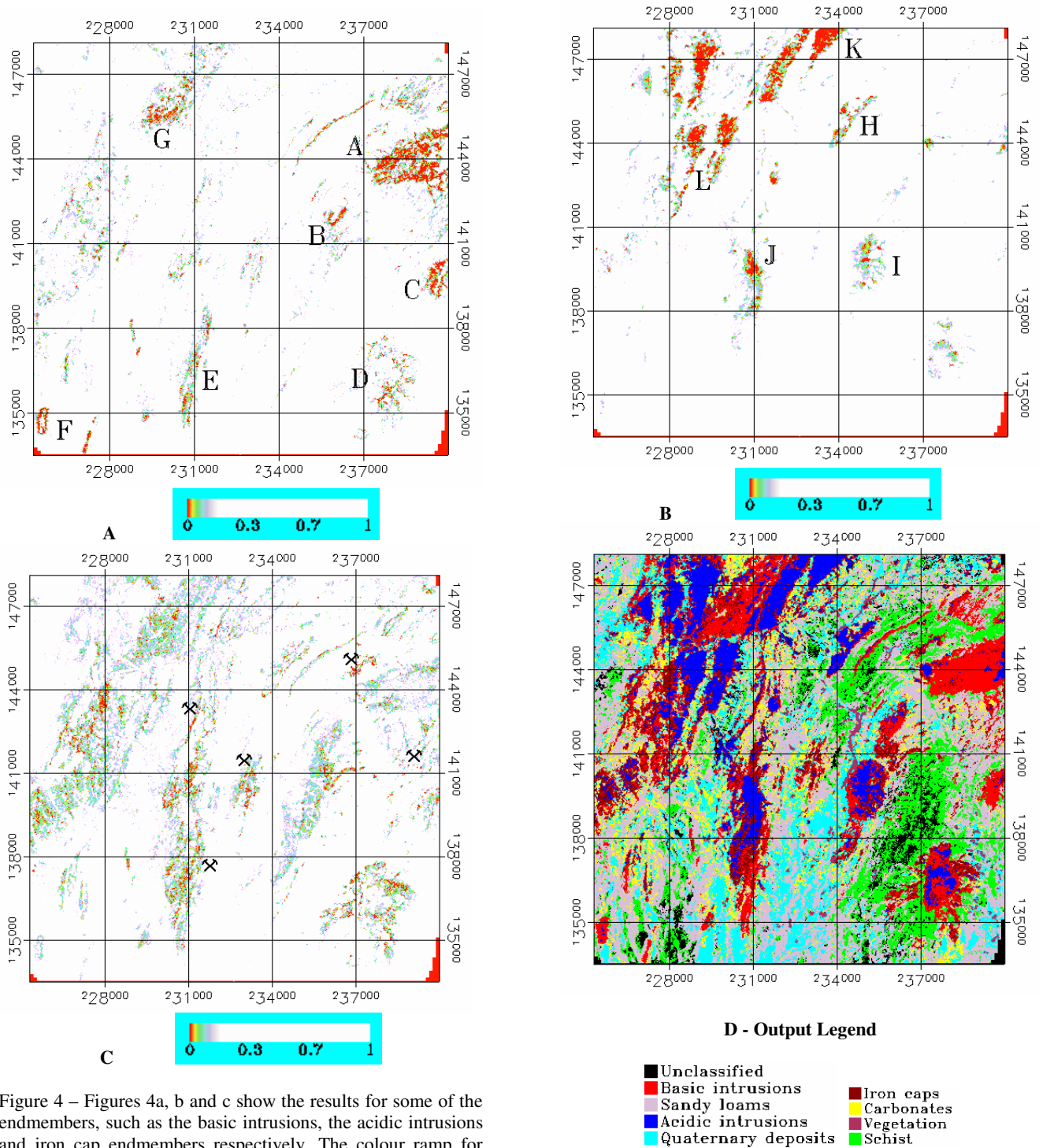Quaternary deposits   Schist

Figure 4 – Figures 4a, b and c show the results for some of the endmembers, such as the basic intrusions, the acidic intrusions and iron cap endmembers respectively. The colour ramp for these endmembers show the values of SAM which are equal or lower than 0.15. Values near 0 (red colour) indicate high similarity between the endmember and image spectra. Figure 4d, is the output classification map with all of the 8 endmembers.

When the eight image endmembers were processed via the SAM algorithm, excellent discrimination between the different endmembers was found. The TM results are relatively accurate with the geological map shown in Figure 1. First of all, the basic volcanic rocks endmember (figure 4a), show the major basic rocks of the study area such as A – K^{at} Kettera, B – S^i Mahjoub, C – K^{at} Ahril, D – Gour es Sefra, E – J.Hadit, F – Menaa el Kahla and G – J. Ahmar. The acidic volcanic rocks endmember also demonstrate good results (figure 4b), as from the identification of the major acidic rocks, such as H – K^{at} Dalaa, I – K^{at} Mirouga, J – K^{at} Aicha, K – K^{at} Hamra and L - K^{at} Bouzelfar. The iron cap endmember gave good results with the identification of areas where they are known to occur. The iron caps were harder to discriminate with SAM because they are relatively narrow in thickness (few meters), but they usually extend for a few kilometers long. For TM, which has a medium spatial resolution, and SAM, which does not consider the sub-pixel, the mixture problem for this unit can cause problems. Also, there is a similarity between the iron caps and the basic intrusions because they are both rich in ferromagnesian minerals, thus their altered surfaces (patina) are similar due to the dark reddish color caused by the alteration of iron oxides and hydroxides.

As shown from the geological map in figure 1, the schist of Sahrlef unit covers most of Central Jebilet. However, when comparing with field observations, a thin layer of Quaternary deposits, which range from conglomerates to rock pebbles and sandy loams, covers most of Central Jebilet. The SAM classification map for TM (figure 5d) clearly shows a higher distribution of Quaternary deposits relative to the schist unit. Because the carbonate endmember was selected in the TM image where the unit was observed in the field and is not shown on geological maps, the output accuracy of this endmember would have to be verified in the field. Finally, the vegetation endmember gave an excellent result due to the semi-arid environment of the study site and sparse vegetation cover, which is very contrast with rocks and bare soils.

3.2 SAM for Quickbird

The SAM results for Quickbird (figure 5) show the SWIR importance for the identification and differentiation of different rock units. The basic and acidic intrusions and iron caps where not clearly recognized with the Quickbird image, as they were with TM. This part of the spectrum is extremely important for mineral and rock discrimination since they have relatively high reflectance and numerous absorption bands caused by minerals. Quickbird did however identify zones where basic intrusions occur such as A – K^{at} Kettera, C – K^{at} Ahril, D – Gour es Sefra, E – J.Hadit and F – Menaa el Kahla and where acidic intrusions occur such as H – K^{at} Dalaa, J – K^{at} Aicha, K – K^{at} Hamra and L - K^{at} Bouzelfar as well as the iron cap of Kettera Mine. Like TM, the Quaternary deposits and sandy loams were widely spread over the study area compared to the schist unit. Vegetation is the endmember that gave the best results because of the near infrared band, which has a high reflectance for vegetation. The overall results for SAM were scattered and most of the geology endmembers were misclassified due to the low spectral dimensions of Quickbird.
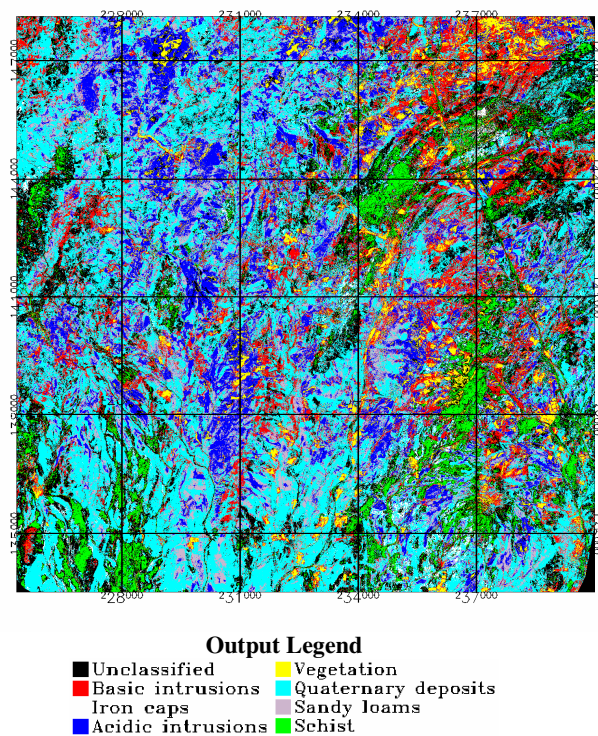

Output Legend

■ Unclassified   ■ Vegetation
■ Basic intrusions   ■ Quaternary deposits
   Iron caps   ■ Sandy loams
■ Acidic intrusions   ■ Schist

Figure 5 – Output classification map for Quickbird.

4. Conclusions

In comparing between high and medium spatial resolutions for the geological mapping of Central Jebilet using SAM algorithm, we have come to the following conclusions. Even if TM has a medium spatial resolution and that sub-pixel contamination from different rocks or cover material is evident while selecting endmembers, it has given good results. On the other hand, Quickbird, which has a fine spatial resolution, gave inadequate results for the surface geology mapping of Central Jebilet. As discussed above, this is caused by the absence of spectral bands in the SWIR, which is the key for mineral exploration with satellite images. The classification map generated with SAM for TM show that this method could effectively be used for geological mapping and potentially be used for exploration in unexplored areas. Whereas Quickbird images would only be helpful for visualizing the study area with great details, locate outcrops in the field and facilitate structural mapping. This demonstrates that for geological mapping, it is much more important to have a high spectral resolution rather than a high spatial resolution. Recent advances in optical remote sensing sensor technology have led to the development of hyperspectral sensors, which acquire images data in many narrow, contiguous spectral bands. Accordingly, each pixel possesses a detailed spectral signature, permitting a more thorough examination than provided by multispectral scanners collecting in a few broad and noncontiguous bands. Certainly, this new technology would be very valuable for geological and mineralogical mapping.

References:

Clark, B.P. (1986). EOSAT Landsat Technical Notes: The New Look-up Tables. Computer Sciences Corp. Silver Spring, MD 20910. Editor, EOSAT Landsat Data User Notes, Lanham, MD, 8 pages.

Crosta, A.P., Sabine, C. and Taranik, J.V. (1998). Hydrothermal Alteration Mapping at Bodie, California, using AVIRIS Hyperspectral Data. Remote Sensing of Environment, Vol. 65, p. 309-319.

De Carvalho, O.A. and Meneses, P.R. (2000). Spectral Correlation Mapper (SCM); An Improvement on the Spectral Angle Mapper (SAM). Summaries of the 9th JPL Airborne Earth Science Workshop, JPL Publication 00-18, 9 p.

Kruse, F.A., Boardman, J.W., Lefkoff, A.B., Heidebrecht, K.B., Shapiro, A.T., Barloon, P.J., and Goetz, A.F.H. (1993). The Spectral Image Processing System (SIPS) – Interactive Visualization and Analysis of Imaging Spectrometer Data. Remote Sensing of Environment, Vol. 44, p.145-163.

Gebbinck, M.S.K. (1998). Decomposition of Mixed Pixels in Remote Sensing Images to Improve the Area Estimation of Agricultural Fields. Ph.D. thesis, Katholieke Universiteit Nijmegen, Veenendaal Universal Press, 165 p.

Hunt, G.R., Salisbury, J.W. and Lenhoff, G.J. (1971). Visible and Near Infrared of Minerals and Rocks III. Oxides and hydroxides. Modern Geology, Vol. 2, p. 195-205.

Hunter, E.L. and Power, C.H. (2002). An Assessment of Two Classification Methods for Mapping Thames Estuary Intertidal Habitats Using CASI Data. International Journal of Remote Sensing, Vol. 23, No. 15, p. 2989-3008.

Huvelin, P. (1970) Carte Géologique et des Minéralisations des Jebilet Centrales au 1/100 000. Sous-secrétariat d'état au commerce, a l'industrie, aux mines et de la géologie. Royaume du Maroc. Notes et Mémoires No 232a.

McCubbin, I., Green, R., Lang, H. and Roberts, D. (1998). Mineral Mapping Using Partial Unmixing at Ray Mine, AZ. Summaries of the 8th JPL Airborne Earth Science Workshop, JPL Publication 97-21, 4 p.

Rowan, L.C. and Mars, J.C. (2003) Lithologic mapping in the Mountain Pass, California area using Advanced Spaceborn Thermal Emission and Reflection Radiometer (ASTER) data. Remote Sensing of Environment, Vol. 84, p. 250-266.

Schwarz, J. and Staenz, K. (2001) Adaptive Threshold for Spectral Matching of Hyperspectral Data. Canadian Journal of Remote Sensing, Vol. 27, No 3, p. 216-224

Small, C. (2003) High Spatial Resolution Spectral Mixture Analysis of Urban Reflectance. Remote Sensing of Environment, Vol. 88, p. 170-186.

Teillet, P.M., Santer, R.P. (1991) Terrain Elevation and Sensor Altitude Dependence in a Semi-Analytical Atmospheric Code. Canadian Journal of Remote Sensing, Vol. 17, No. 1, January, 1991

Van der Meer, F., Vasquez-Torres, M., and Van Dijk, P.M. (1997). Spectral Characterization of Ophiolite Lithologies in the Troodos Ophiolite Complex of Cyprus and its Potential in Prospecting for Massive Sulphide Deposits. International Journal of Remote Sensing, Vol. 18, No.6, p. 1245-1257.

Wu, C. and Murray, A.T. (2003) Estimating Impervious Surface Distribution by Spectral Mixture Analysis. Remote Sensing of Environment, Vol. 84, p. 493-505.

Yuhas, R.H., Goetz, A.F.H., and Boardman, J.W. (1992). Discrimination Among Semi-Arid Landscape Endmembers Using the Spectral Angle Mapper (SAM) Algorithm. Summaries of the 4th JPL Airborne Earth Science Workshop, JPL Publication 92-41 pp.147-149